COMPARISON OF AREAS IN SHADOW FROM IMAGING AND ALTIMETRY IN THE NORTH POLAR REGION OF MERCURY AND IMPLICATIONS FOR POLAR ICE DEPOSITS. Ariel N. Deutsch[1], Nancy L. Chabot[2], Erwan Mazarico[3], Carolyn M. Ernst[2], James W. Head[1], Gregory A. Neumann[3], and Sean C. Solomon[4,5], [1]Department of Earth, Environmental and Planetary Sciences, Brown University, Providence, RI 02912, USA (ariel_deutsch@brown.edu), [2]The Johns Hopkins University Applied Physics Laboratory, Laurel, MD 20723, USA, [3]NASA Goddard Space Flight Center, Greenbelt, MD 20771, USA, [4]Lamont-Doherty Earth Observatory, Columbia University, Palisades, NY 10964, USA, [5]Department of Terrestrial Magnetism, Carnegie Institution of Washington, Washington, DC 20015, USA.

Introduction: Through a combination of Earth-based radar observations, spacecraft data, and thermal modeling, evidence has grown to support the hypothesis that Mercury hosts water-ice deposits in its polar regions. Radar observations revealed radar-bright materials near Mercury's poles in areas thought never to receive direct sunlight [1]. The MErcury Surface, Space ENvironment, GEochemistry, and Ranging (MESSENGER) spacecraft confirmed that the polar deposits are in areas of permanent or persistent shadow [2], measured higher hydrogen concentrations in Mercury's north polar region [3], and measured topography with which thermal models indicated that permanently shadowed regions near Mercury's north pole provide environments capable of hosting water-ice deposits that are stable on geologic timescales [4]. MESSENGER's active reflectance measurements [5] and imaging of radar-bright deposits in shadowed polar craters [6] revealed both high- and low-reflectance surfaces, interpreted to be exposed water ice at the surface or layers of organic-rich materials, formed as lag deposits, which insulate water ice beneath.

Determining the precise areas of permanent shadow on Mercury is critical for interpreting the distribution of water ice and other volatiles in polar deposits, and MESSENGER's complete datasets enable the best determination to date. In this work, we map shadow in Mercury's north polar region from 65°N to 90°N using two independent methods. From images acquired by the Mercury Dual Imaging System (MDIS), we map any area that remained in shadow in all images as a region of "persistent shadow." From topographic data acquired by the Mercury Laser Altimeter (MLA), we model areas of permanent shadow. We compare the spatial distribution of regions of shadow to that of deposits identified from Earth-based radar observations, and we discuss the implications for water ice on Mercury.

MDIS Data Set and Methodology: During its more than four years of orbital operations, MDIS repeatedly imaged Mercury's north polar region, capturing the surface under a range of illumination conditions that expose the planet in different degrees of shadow. We utilized 16,207 wide-angle camera images taken with the 750-nm G filter (5.1-nm bandwidth) and the 700-nm B filter (600-nm bandwidth) to identify regions of persistent shadow from 65°N to the pole at 200 m/pixel. The images were separated into areas of illumination and shadow, automated by thresholding each image based on the digital value of individual pixels, following earlier methods [2].

MLA Data Set and Methodology: MLA acquired more than 26 million altimetric range measurements of Mercury's surface during MESSENGER's operation, primarily in the northern hemisphere. From this dataset, a digital elevation model (DEM) of Mercury's north polar region was constructed at a pixel scale of 500 m and was used for modeling solar illumination conditions. As was done previously [7], the solar illumination was computed at every hour over a time period of 20 Mercury solar days, or ~9.6 Earth years. Pixels that were not illuminated during the simulation period were considered to be in permanent shadow; this assumption is justified because Mercury's obliquity is stabilized by the planet's spin-orbit resonance and has a very small value at <0.04°, much smaller than the Sun's angular radius [8]. Our simulations are based on Mercury's current orbital parameters, and thus what we determine as "permanent shadow" may not apply over long timescales. Given Mercury's fixed obliquity [9], we verified that a change in eccentricity does not substantially change the modeled region of permanent shadow.

North Polar Shadow Maps: The MDIS- and MLA-derived shadow maps show strong agreement in the spatial distribution of shadows (Fig. 1). Both maps indicate that ~1.1% of the surface between 65°N to 90°N is in steady shadow, similar to the ~1% that was calculated for the region between 65°N and 85°N from MDIS images after the first year of orbital data [2]. The percentage of persistently and permanently shadowed terrain increases with latitude, as expected because of Mercury's low obliquity. In the region from 80°N to 90°N, ~4.7% of the surface is in persistent shadow in the map derived from imagery, and ~5.8% is in permanent shadow in the map derived from altimetry. These values are similar to the ~4.5% and ~5.6% of shadowed surface modeled for areas within 10° of

latitude of the Moon's north and south poles, respectively [7].

Comparison with Radar Data: The radar image that was used for comparison with the shadow maps was a combination of Figures 3b and 4 presented by Harmon et al. [1]. The first was constructed from a weighted sum of 12 groups of Arecibo S-band (12.6 cm wavelength) observations, acquired over a span of six years, to minimize radar shadowing effects. Because this data set is geographically limited to the latitudes closest to the pole, we supplemented these data with the large-scale radar view provided in Figure 4 to cover the region from 65°N to 90°N. To account for noise in the radar data, we set a threshold of four standard deviations of the noise [1]. With this choice, radar-bright material covers ~0.38% of the surface from 65°N to 90°N and ~2.2% from 80°N to 90°N.

The strong spatial agreement between areas in Mercury's north polar region with persistent and permanent shadow and radar-bright deposits is shown in Fig. 1. In the region between 80°N and 90°N, ~79% of the radar-bright deposits coincide with areas of persistent shadow determined from images, and ~80% with areas of permanent shadow determined from topography. We attribute the remaining ~20% to limitations in our methodologies, as the non-coincident radar-bright material is found either within 5 km of large areas of mapped persistent and permanent shadow or inside small craters with diameters ≤6 km.

Interestingly, in the region from 80°N to 90°N, only ~46% of the area of persistent shadow and ~43% of that of permanent shadow contain radar-bright materials. In both the MDIS- and MLA-derived maps, there are large shadowed regions that do not host substantial radar-bright deposits, as can be seen in Fig. 1 for craters Burke, Sapkota, and Yamada. It is possible that these craters and other such shadowed regions do not host water ice, or that they host water-ice deposits that are covered by thicker lag deposits that mask radar returns from the underlying ice, or alternatively that they host water ice that was not detected by the Earth-based radar observations because of visibility or sensitivity limits. There is a longitudinal dependence of the locations of large (≥10 km diameter) craters with areas of persistent or permanent shadow that lack radar-bright deposits, but this distribution is not controlled by the longitudes of Mercury's hot and cold poles.

Finally, although most small (<10 km diameter) simple craters do not host radar-bright materials, many small secondary craters from Prokofiev do. These secondary craters may be shallower than primary craters of the same diameter and provide a thermal environment that allows water ice to be stable on geologic timescales [10].

References: [1] Harmon J. K. et al. (2011) *Icarus*, 211, 37–50. [2] Chabot N. L. et al. (2013) *JGR Planets*, 118, 26–36. [3] Lawrence D. J. et al. (2013) *Science*, 339, 292–296. [4] Paige D. A. et al. (2013) *Science*, 339, 300–303. [5] Neumann G. A. et al. (2013) *Science*, 339, 296–300. [6] Chabot N. L. et al. (2014) *Geology*, 42, 1051–1054. [7] Mazarico E. et al. (2011) *Icarus*, 211, 1066. [8] Margot J. L. (2009) *Celest. Mech. Dyn. Astron.*, 105, 329–336. [9] Yseboodt M. and Margot J. L. (2006) *Icarus*, 181, 327–337. [10] Ernst C. M. et al. (2014) *LPS*, 45, abstract 1238.

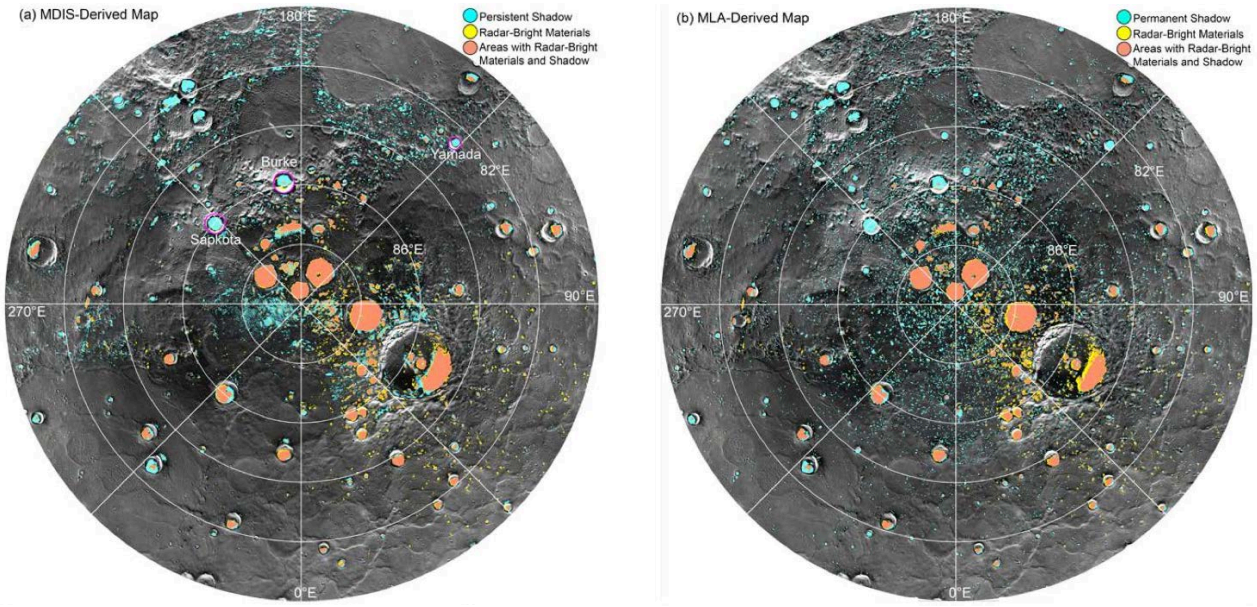

Figure 1. Shadowed regions displayed on a mosaic of MESSENGER images from 80°N to 90°N in polar stereographic projection. Areas shadowed in (a) all MDIS images or (b) the MLA model are shown in cyan, radar-bright deposits in yellow, and areas with both shadow and radar-bright materials are in coral.